Kinetics of the Structural Transition of Muscle Thin Filaments Observed by Fluorescence Resonance Energy Transfer†

Yuji Shitaka,‡ Chieko Kimura,‡ Takayoshi Iio,§ and Masao Miki*,‡

Department of Applied Chemistry and Biotechnology, Fukui University, 3-9-1 Bunkyo, Fukui 910-8507, Japan, and Physics Section, Division of Material Science, Graduate School of Science, Nagoya University, Chikusa-ku, Nagoya 464-8602, Japan

Received April 12, 2004; Revised Manuscript Received May 26, 2004

ABSTRACT: Fluorescence resonance energy transfer showed that troponin-I changes the position on an actin filament corresponding to three states (relaxed, closed, and open) of the thin filament (Hai et al. (2002) *J. Biochem. 131*, 407−418). In combination with the stopped-flow method, fluorescence resonance energy transfer between probes attached to position 1, 133, or 181 of troponin-I and Cys-374 of actin on reconstituted thin filaments was measured to follow the transition between three states of the thin filament. When the free Ca^{2+} concentration was increased, the transition from relaxed to closed states occurred with a rate constant of ∼500 s^{-1}. For the reverse transition, the rate constant was ∼60 s^{-1}. When myosin subfragment-1 was dissociated from thin filaments in the presence of Ca^{2+} by rapid mixing with ATP, the transition from open to closed states occurred with a single rate constant of ∼300 s^{-1}. Light-scattering measurements showed that the ATP-induced myosin subfragment-1 dissociation occurred with a rate constant of ∼900 s^{-1}. In the absence of Ca^{2+}, the transition from open to relaxed states occurred with two rate constants of ∼400 and ∼80 s^{-1}. These transition rates are fast enough to allow the spatial rearrangement of thin filaments to be involved in the regulation mechanism of muscle contraction.

In striated muscle, the interaction of myosin with actin is regulated by tropomyosin (Tm)[1] and troponin (Tn) on actin filaments in response to a change in Ca^{2+} concentration from approximately 10^{-7} to 10^{-5} M (*1*). Tm, an extended coiled-coil dimer, binds end-to-end along the actin filament and covers seven actin monomers (*2*). Tn is a complex of three proteins: troponin-C (TnC), troponin-I (TnI), and troponin-T (TnT). The binding of Ca^{2+} to TnC induces a series of conformational changes in the other components of the thin filament, which allow the effective association of myosin to actin and force generation. Although numerous studies have characterized the interaction between the thin filament proteins to deduce how the Ca^{2+}-triggering signal is propagated from TnC to the rest of the thin filament (*3*−*7*), the mechanism of this regulatory process is still not well understood. Early explanation for the regulation mechanism is that thin filaments have two states, "on" and "off" and the two states are regulated by tropomyosin movement between switched-on and switched-off locations on thin filaments depending on Ca^{2+} concentrations (*8*, *9*). On the other hand, biochemical studies of regulation demonstrated that Ca^{2+} regulates actomyosin ATPase by controlling a kinetic transition (from a weak to a strong binding form of myosin) and not by controlling the binding of myosin to actin. They also showed that the strong binding of myosin to actin modulates this transition through its effect on the thin filament (*5*−*7*). These cannot be explained by the simple, steric blocking view of regulation. Instead of a two-state model based on Ca^{2+}-induced on−off switching, kinetic measurements proposed a three-state model (*10*−*12*). In this model, a thin filament exists in rapid equilibrium between three states, blocked, closed, and open. The equilibrium between the blocked and closed states is calcium-sensitive, and strong myosin subfragment-1 (S1) binding stabilizes the open state. Recent structural studies with X-ray diffraction and three-dimensional image reconstruction of electron micrographs (3D-EM) have led to a new model in which Tm moves between three and not two distinct states (*13*, *14*). However, the interpretations of these measurements have been questioned because they do not take into consideration the presence of Tn and possible changes in its structure with Ca^{2+} (*15*).

Fluorescence resonance energy transfer (FRET) has been used as a spectroscopic ruler in the range of several tens angstroms (*16*), and has been extensively applied for structural studies of muscle proteins (*17*, *18*). This method is especially valuable for detecting a small conformational

† This study was performed through the Special Coordination Funds of the Ministry of Education, Culture, Sports, Science, and Technology of the Japanese Government.

* To whom correspondence should be addressed: Department of Applied Chemistry and Biotechnology, Bunkyo 3-9-1, Fukui, 910-8507 Japan. Telephone: +81-776-27-8786. Fax: +81-776-27-8747. E-mail: masao@acbio.fukui-u.ac.jp.

‡ Fukui University.

§ Nagoya University.

[1] Abbreviations: Tm, tropomyosin; Tn, troponin; TnC, troponin-C; TnI, troponin-I; TnT, troponin-T; S1, myosin subfragment-1; 3D-EM, three-dimensional image reconstruction of electron micrographs; FRET, fluorescence resonance energy transfer; IAEDANS, 5-(2-iodoacetylaminoethyl)aminonaphthalene 1-sulfonic acid; DABMI, 4-dimethylaminophenylazophenyl 4′-maleimide; DTT, dithiothreitol; AEDANS-1-Tn, troponin complex labeled at Cys-1 of a single-cysteine mutant TnIG1C with IAEDANS; AEDANS-133-Tn, troponin complex labeled at Cys-133 of TnI with IAEDANS; AEDANS-181-Tn, troponin complex labeled at Cys-181 of a single-cysteine mutant TnIS181C with IAEDANS; DAB-F-actin, F actin labeled at Cys-374 with DABMI.

10.1021/bi0492713 CCC: $27.50
Published on Web 07/29/2004

change of several angstroms, because the transfer efficiency is a function of the inverse of the sixth power of the distance between probes. Furthermore, fluorescence donor and acceptor molecules are specifically attached to proteins so that assignment of the conformational change is direct. Using this method, several attempts have been made to detect a conformational change of thin filaments. FRET between probes attached to TnI and actin showed a significant extent of movement of TnI on the thin filament with changes in Ca^{2+} concentration (*19*−*23*). Recent FRET measurements showed that TnI has three positions on thin filaments corresponding to the three states of thin filaments, "relaxed" or "locked", "closed", and "open" states (*24*). The term of "locked" state has been used for "relaxed" state in our regulation model, instead of "blocked" state used in the original three-state model. The binding of Ca^{2+} to Tn induces the transition from relaxed to closed states, and the strong binding of myosin heads to actin leads to the open state whether Ca^{2+} is present or not. D234Tm, in which three of seven repeats (49−167 amino acid residues) have been deleted, inhibits actomyosin−MgATPase even in the presence of Ca^{2+} (*25*). FRET measurement showed that the transition of TnI to the "open" position on the thin filament reconstituted with D234Tm was impaired, indicating that the three positions of TnI on the thin filament are closely related to the regulation mechanism (*24*). Furthermore, FRET demonstrated that TnT also moves significantly on the thin filament corresponding to the three states (*26*).

To study the kinetics of the conformational change of the thin filament, several stopped-flow measurements have been carried out (*11*, *21*, *27*−*29*). Fluorescent probes were attached to Tm or actin, and the time course of fluorescence intensity change was traced (*11*, *27*−*29*). Fluorescence intensities of probes on Tm or actin respond primarily to the binding of activating cross bridges but not to the change in Ca^{2+} concentrations. On the other hand, FRET between probes on TnI and actin showed that the position of TnI on F-actin filament corresponds well to the three states of the thin filament (*24*). In our previous report (*21*), Cys-133 of TnI and Lys-61 of actin were labeled with the fluorescence energy donor and energy acceptor, respectively, and the time course of TnI movement upon Ca^{2+}-binding or release was monitored by FRET. In the present study, the N or C terminus of TnI in addition to Cys-133, by using mutant TnI, was selectively labeled with 5-(2-iodoacetylaminoethyl)-aminonaphthalene 1-sulfonic acid (IAEDANS) and Cys-374 of actin was labeled with 4-dimethyl-aminophenylazophenyl 4′-maleimide (DABMI). FRET between these probes was measured in combination with the stopped-flow apparatus to determine the transition rates between three states of thin filaments. The rate of S1 binding to or dissociating from regulated thin filaments, monitored by light scattering, was compared with the rate of transition between three states.

MATERIALS AND METHODS

Phalloidin from *Amantina phalloides* was purchased from Sigma. IAEDANS and DABMI were purchased from Molecular Probes. All other chemicals were of analytical grade.

Proteins. Actin, S1, and Tn were prepared from rabbit skeletal muscle as reported previously (*19*). αTm was extracted from rabbit hearts as previously reported (*19*). To prepare single-cysteine mutants TnIG1C and TnIS181C, we started with a cDNA for a Cys-less TnI mutant (C48A, C64A, and C133S) (*30*). To construct TnIS181C, mutagenesis was carried out on a pTV118 template using standard protocols of Sculptor in vitro mutagenesis system (Amersham). The oligonucleotide used for TnI (S181C) mutation was as follows (the mutant codon is underlined): G TCC GAG TGC TAG GCC G. The resultant plasmid for expression of the mutant TnI has been designed as pET-TnIS181C. To construct TnIG1C, a 0.6-kbp *Bgl*I-*Eco*RI fragment containing the Cys-less TnI-coding sequence was inserted into the *Nco*I and *Eco*RI sites of pET23d between the *Nco*I and *EcoR*I sites together with a pair of oligonucleotides. The oligonucleotides, which fill the gap between the *Nco*I and *Bgl*I sites, were designed to replace Glu-1 to cysteine as follow: CATGTGTGATGAAGAAAAACGCAACCGTGCCATCA. TnIG1C and TnIS181C were expressed in BL21 (DE3) pLysS (Novagen) according to the method of Kluwe et al. (*30*). Expressed single-cysteine TnI mutants went into the insoluble fraction. Pellets were collected by centrifugation at 10000*g* for 30 min and resuspended in 50 mM Tris-HCl (pH 8.0), 8% sucrose, 5% Triton X-100, and 50 mM EDTA. The pellets were resuspended in 6 M urea, 50 mM Tris-HCl (pH 8.0), 1.0 mM EDTA, and 1 mM NaN_3 (solution U), including the inhibitor cocktail (Roche Diagnostics, a tablet per 50 mL of solution). The supernatant was applied to the Q-sepharose column (Pharmacia LKB Biotechnology, 2.5 × 10 cm) equilibrated with solution U. The flow-through fraction was then applied to the S-sepharose column (Pharmacia LKB Biotechnology, 2.5 × 12 cm) equilibrated with solution U. Single-cysteine TnI mutants were eluted with a 0.5 M NaCl step. The fraction containing single-cysteine TnI mutants were dialyzed against 25 mM phosphate buffer (pH 7.0), 0.5 M KCl, and 1 mM $CaCl_2$ and then applied to the TnC affinity column (Bio-rad, 2.5 × 3 cm) equilibrated with the same buffer. The single-cysteine TnI mutants were eluted from the column with 6 M urea, 25 mM phosphate buffer (pH 7.0), and 1 mM EGTA.

Ternary Tn Complexes with AEDANS-Labeled TnI. The Tn complexes labeled with IAEDANS at positions 1 (AEDANS-1-Tn), 133 (AEDANS-133-Tn), and 181 (AEDANS-181-Tn) of TnI were prepared as follows. Single-cysteine mutants (TnIG1C and TnIS181C) were incubated with a 10-fold molar excess of IAEDANS in 0.5 M KCl and 20 mM phosphate buffer (pH 7.0) for 24 h at 25 °C. The reaction was terminated by the addition of 10 mM dithiothreitol (DTT), and the sample solution was dialyzed against 5 mM Tris-HCl (pH 8.0) and 0.4 M KCl exhaustively to remove free IAEDANS. Cys-133 on TnI was specifically labeled with IAEDANS in the Tn complex as reported previously (*22*). Tn subunits including TnI mutants were combined in a solution containing 6 M urea, 0.4 M KCl, 1 mM $CaCl_2$, 1 mM DTT, and 20 mM Tris-HCl (pH 8.0). TnI mutants, TnC, and TnT were mixed in a molar ratio of 1:1:1.2, respectively. The mixture was then dialyzed consecutively against 1 M, 0.5 M, 0.3 M, 0.1 M, and 30 mM KCl solutions, each containing 1 mM $CaCl_2$, 10 mM β-mercaptoethanol, and 20 mM Tris-HCl (pH 8.0). After dialysis, the protein solution was clarified by centrifugation and applied to the Hitrap-Q column (Pharmacia) equilibrated with 30 mM KCl, 1 mM $CaCl_2$, and 20 mM Tris-HCl (pH 8.0). The ternary complex was eluted with a linear gradient of 30−

300 mM KCl in 1 mM $CaCl_2$ and 20 mM Tris-HCl (pH 8.0). Fractions containing the pure complex were identified by SDS gel electrophoresis. The purified Tn complex was dialyzed against 5 mM Tris-HCl (pH 8.0) and 0.1 M KCl. Actin was labeled at Cys-374 with DABMI as described previously (*24*). The absorption coefficient of 24 800 M^{-1} cm^{-1} at 460 nm for DABMI (*31*) was used for the determination of labeling ratios. The typical ratio was 1.0 for DAB−actin. The absorption coefficient of 6100 M^{-1} cm^{-1} at 337 nm for IAEDANS (*32*) was used for the determination of the labeling ratios. The typical labeling ratios were 1.0 for AEDANS-1-Tn, 0.96 for AEDANS-133-Tn, and 0.8 for AEDANS-181-Tn. For fluorescence measurements, including stopped-flow measurements, equimolar phalloidin to actin was added to stabilize the actin filament.

The following extinction coefficients were used to calculate protein concentrations: $A_{290nm} = 0.63$ $(mg/mL)^{-1}$ cm^{-1} for G actin, $A_{280nm} = 0.75$ for S1, 0.235 for Tm, 0.45 for Tn, 0.18 for TnC, 0.458 for TnT, and 0.40 $(mg/mL)^{-1}$ cm^{-1} for TnI and mutant TnI. Relative molecular masses of 42 000 for actin, 115 000 for S1, 66 000 for Tm, 70 000 for Tn, 18 000 for TnC, 21 000 for TnI, and 31 000 for TnT were used.

Spectroscopic Measurements. Absorption was measured with a Hitachi U2000 spectrophotometer. Steady-state fluorescence was measured with a Perkin−Elmer LS50B fluorometer. The temperature was maintained at 20 °C. Sample cells were placed in a thermo-stated cell holder.

FRET. The efficiency E of resonance energy transfer between probes was determined by measuring the fluorescence intensity of the donor in the presence (F_{DA}) and absence (F_{D0}) of the acceptor, as given by

$$E = 1 - F_{DA}/F_{D0} \quad (1)$$

According to Förster's theory (*16*, *33*), the efficiency is related to the distance (R) between probes and to Förster's critical distance (R_0) at which the transfer efficiency is equal to 50%.

$$E = R_0^6/(R^6 + R_0^6) \quad (2)$$

R_0 can be obtained (in nanometers) from

$$R_0^6 = (8.79 \times 10^{-11}) n^{-4} \kappa^2 Q_0 J \quad (3)$$

where n is the refractive index of the medium, taken to be 1.4, κ^2 is the orientation factor, Q_0 is the quantum yield of the donor in the absence of the acceptor, and J is the spectral overlap integral between the donor emission $F_D(\lambda)$ and the acceptor absorption $\epsilon_A(\lambda)$ spectra, defined by

$$J = \int F_D(\lambda) \epsilon_A(\lambda) \lambda^4 \, d\lambda / \int F_D(\lambda) \, d\lambda \quad (4)$$

The quantum yield was determined by the comparative method using quinine sulfate in 0.1 N H_2SO_4 as the standard, which has an absolute quantum yield of 0.70 (*34*). κ^2 was taken as $^2/_3$ for the calculation of distances. The decrease in the fluorescence intensity because of inner-filter effects was corrected with

$$F_{corr} = F_{obs} \times 10^{(A_{ex} + A_{em})/2} \quad (5)$$

where A_{ex} and A_{em} are absorbencies of the samples at the excitation and emission wavelengths, respectively.

Stopped-Flow Measurements. Kinetic measurements were performed with an Applied Photophysics Ltd. model SX.18 MV stopped-flow spectrofluorometer. The excitation monochromator was set to 340 nm for fluorescence or 500 nm for scattering measurements, and the light from 420 to 540 nm was collected through a broad band cut filter (Chroma Technology Co.) placed at the emission side. The instrumental dead time was 1.63 ms under the present experimental conditions. For each experiment, the reaction curves are the average of 10 reaction traces. The data were fitted with a nonlinear least-squares procedure to a single- or double-exponential expression from which the rate constants were calculated. Prior to the stopped-flow experiments, the pH of the protein sample solutions were adjusted at 7.5, and the pH of the mixing buffer solutions (Ca^{2+} or EGTA solutions) was adjusted by KOH to give the value of 7.5 after rapid mixing with the protein solutions. Data sets were fit to the single- and double-exponential equation with floating end point, using the Applied Photophysics Ltd SX.18MV Kinetic Spectrometer Workstation software.

Other Methods. ATPase activity was measured by the method of Tausky and Shorr (*35*). The biological activity of the labeled troponin was assayed by determining the Ca^{2+}-dependent regulation of actoS1 ATPase activity in a fully reconstituted system.

RESULTS

To test whether the Tn complexes reconstituted with the AEDANS-labeled TnI retain the essential property of being able to participate in the calcium regulation process, the ATPase activity of reconstituted thin filaments composed of S1, Tn, Tm, and F actin were measured in the presence and absence of Ca^{2+}. Measurements were performed at 25 °C in 10 mM KCl, 4 mM $MgCl_2$, 2.0 mM ATP, 20 mM Tris-HCl (pH 7.6), 0.5 mM DTT, and 50 μM $CaCl_2$ (+Ca^{2+} state) or 1 mM EGTA (−Ca^{2+} state). Protein concentrations were 24 μM F actin, 5 μM Tm, 5 μM Tn, and 0.52 μM S1. The regulatory capacity value is defined as $1 - (Act_{-Ca}/Act_{+Ca})$, where Act_{-Ca} and Act_{+Ca} are the Mg−ATPase activities in the absence and presence of Ca^{2+}, respectively. The values for wild-type TnI, labeled TnI, mTnI (G1C), and mTnI (S181C) were determined to be 0.88, 0.95, 0.92, and 0.83, respectively, which showed that the mutation and the labeling of AEDANS did not significantly impair the regulatory activity of Tn.

Steady-State Fluorescence Measurements. FRET between AEDANS-1-Tn and DAB-F-actin was measured in the same procedure as reported previously (*24*). The ratio of donor quenching was measured by titrating AEDANS-1-Tn/Tm with DAB-F-actin in the presence and absence of Ca^{2+} at 20 °C (Figure 1A). For correction of the fluorescence intensity change of AEDANS-1-Tn upon binding to an actin filament, the same amount of nonlabeled F actin was added to AEDANS-1-Tn/Tm in the presence and absence of Ca^{2+} as the reference, and the ratio of these fluorescence intensities was taken as the relative fluorescence intensity. The solvent conditions were 30 mM KCl, 2 mM $MgCl_2$, 20 mM Tris-HCl (pH 7.6), 1 mM NaN_3, and 50 μM $CaCl_2$ (buffer A_{+Ca}) or 1 mM EGTA (buffer A_{-Ca}) with 0.1 mM ATP. The

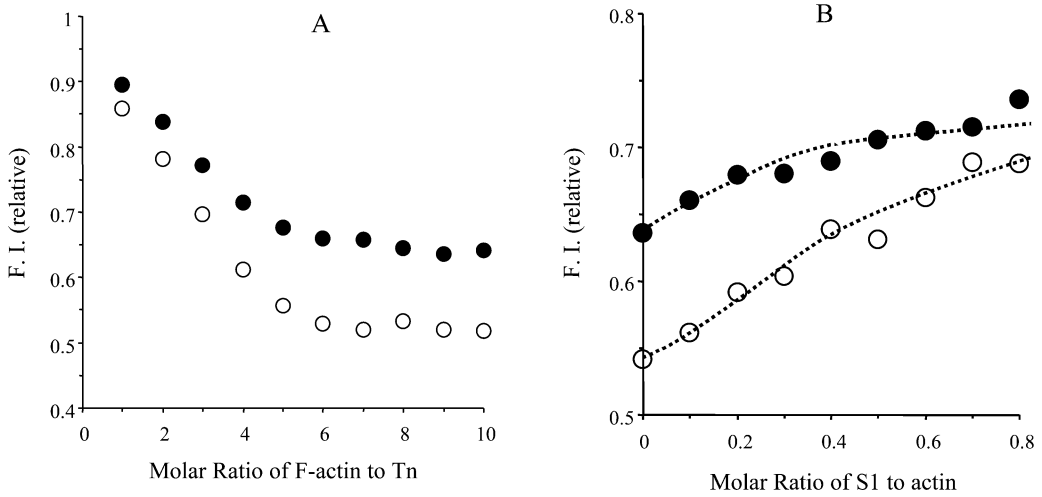

FIGURE 1: Relative fluorescence intensities of AEDANS-1-Tn (● for the $+Ca^{2+}$ and ○ for the $-Ca^{2+}$ states) (A) in the Tn−Tm complex versus the molar ratio of DAB-F-actin/Tn, and (B) in the reconstituted thin filament versus the molar ratio of S1/actin. Values were obtained after correction of the inner-filter effects according to eq 5. Excitation was at 340 nm, and emission was measured at 490 nm. (A) Concentrations of AEDANS-1-Tn and Tm were 0.7 and 0.7 μM, respectively. (B) The concentrations of F actin, Tm, and Tn were 5.4, 0.7, and 0.7 μM, respectively. Fluorescence measurements were carried out after hydrolysis of contaminant ATP (less than 10 μM) by S1.

relative fluorescence intensity decreased in the actin/Tn molar ratio range up to 7 and became almost constant in the range over 7. The fluorescence intensity of AEDANS-1-Tn on thin filaments was not sensitive to the Ca^{2+} concentration in the absence of the acceptor, but in the presence of the acceptor, it showed a significant difference between in the presence and absence of Ca^{2+}. From the saturation points, the energy-transfer efficiencies were calculated to be 0.38 ± 0.02 in the presence of Ca^{2+} and 0.48 ± 0.02 in the absence of Ca^{2+}, corresponding to the distances of 41.5 ± 0.5 and 38.8 ± 0.5 Å, respectively.

The effect of S1 binding on FRET was examined in buffer $A_{\pm Ca}$. A small volume of a concentrated S1 solution was added stepwise. The addition of S1 increased the donor fluorescence intensity for both the $+Ca^{2+}$ and $-Ca^{2+}$ states as in the case of FRET between probes attached to Cys-133 of TnI and to Cys-374 or Gln-41 of actin reported previously (*24*) (Figure 1B). To correct the dilution effects and fluorescence changes of AEDANS-1-Tn induced by the addition of S1, the sample containing nonlabeled F actin instead of DAB-F-actin was used as a reference and the ratio of fluorescence intensities was taken. The relative fluorescence intensities showed a large difference between the presence and absence of Ca^{2+} before the addition of S1 and increased regardless of whether Ca^{2+} is present or not, as the molar ratio of S1 to actin increased. The distance between Cys-1 of TnI and Cys-374 of actin on reconstituted thin filaments was calculated to be 45.6 ± 1.1 Å in the S1-induced state.

FRET between AEDANS-181-Tn and DAB-F-actin was also measured under the same experimental conditions. The fluorescence intensity of AEDANS-181-Tn on thin filaments was not sensitive to the Ca^{2+} concentration in the absence of the acceptor, but in the presence of the acceptor, it also showed a significant difference between in the presence and absence of Ca^{2+}. The transfer efficiencies and distances are summarized in Table 1. Results suggest that not only near the inhibitory region of TnI (Cys-133) but also the N- and C-termini of TnI (Cys-1 and Cys-181) change their positions on the thin filament corresponding to three states of the thin filament, although the extent of the distance change is different from each other.

Table 1: Distances between Probes Attached to Tn and Actin (Cys-374) in Reconstituted Thin Filament in the Presence and Absence of Ca^{2+} Ions and S1 Observed by Steady-State Fluorescence

donor site (TnI)	$R_0(^2/_3)$ (Å)		Ca^{2+}	E	$R(^2/_3)$ (Å)
TnI G1C	38.4		−	0.48 ± 0.02	38.8 ± 0.5
			+	0.38 ± 0.02	41.5 ± 0.5
		+S1	±	0.26 ± 0.03	45.6 ± 1.1
TnI Cys133[a]	38.1		−	0.75 ± 0.02	31.7 ± 0.6
			+	0.42 ± 0.02	40.2 ± 0.6
		+S1	±	0.20 ± 0.03	47.9 ± 1.5
TnI S181C	37.0		−	0.43 ± 0.02	38.9 ± 0.6
			+	0.29 ± 0.01	42.9 ± 0.4
		+S1	±	0.26 ± 0.02	44.0 ± 0.8

[a] From Hai et al. (*24*).

Kinetics of Ca^{2+}-Induced Movement of TnI. FRET in combination with the stopped-flow method was used to measure transition rates between the locked and closed states. The change in the energy transfer efficiency after changing the solvent conditions from $-Ca^{2+}$ to $+Ca^{2+}$ (or vice versa) was monitored by the donor-fluorescence intensity. Figure 2 shows the time courses of fluorescence intensity change of AEDANS-1-Tn in thin filaments reconstituted with DAB-F-actin. The thin filament in 30 mM KCl, 2 mM $MgCl_2$, 1 mM NaN_3, and 20 mM MOPS at pH 7.5 (buffer F) with 0.5 mM EGTA (buffer F_{-Ca}) or 0.1 mM $CaCl_2$ (buffer F_{+Ca}) was rapidly mixed with the same volume of buffer F containing 4 mM $CaCl_2$ or 3.75 mM EGTA, respectively, at 20 °C. After the solvent condition was changed from $-Ca^{2+}$ to $+Ca^{2+}$ (curve A), fluorescence intensity increased very rapidly and reached a final fluorescence level at around 10 ms after the flow stop. The observed fluorescence change was fitted by a single-exponential curve with the rate constant of 389 ± 73 s^{-1}. After the solvent was changed from $+Ca^{2+}$ to $-Ca^{2+}$ (curve C), fluorescence intensity decreased much slower than that from $-Ca^{2+}$ to $+Ca^{2+}$ with a single-exponential type as 75.1 ± 7.7 s^{-1}. Curves B and D show the time courses of fluorescence intensity without changing the Ca^{2+} concentrations. Time courses of fluorescence intensity change of

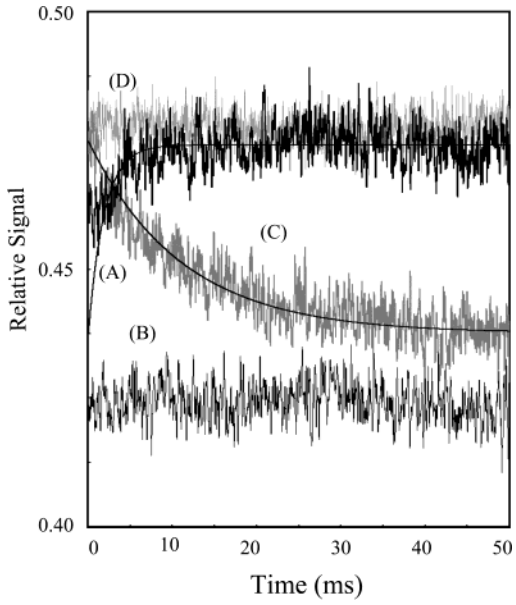

FIGURE 2: Stopped-flow traces for the Ca^{2+}-induced TnI movement on the reconstituted thin filament. The solution containing 4.7 μM F actin, 0.67 μM Tm, and 0.64 μM Tn in buffer F_{-Ca} (A and B) or F_{+Ca} (C and D) were rapidly mixed with the same volume of buffer F + 4 mM $CaCl_2$ (A) or 3.75 mM EGTA (C) at 20 °C. For B and D, Ca^{2+} concentrations were not changed to see the initial level of A and C. The best-fit exponential curve to each trace was superimposed.

Table 2: Rate Constants of the Transition between States of a Thin Filament Induced by Ca^{2+} Binding/Dissociation

donor site of TnI	from $-Ca^{2+}$ to $+Ca^{2+}$ (s^{-1})	from $+Ca^{2+}$ to $-Ca^{2+}$ (s^{-1})
TnI G1C	389 ± 73	75.1 ± 7.7
TnI Cys133[a]	530 ± 170	43 ± 5
TnI S181C	534 ± 87	60.6 ± 2.0

[a] From Miki and Iio (*21*).

AEDANS-181-Tn in thin filaments reconstituted with DAB-F-actin were also followed after changing the solvent conditions from $-Ca^{2+}$ to $+Ca^{2+}$ (or vice versa). The fluorescence intensity changes were fitted by a single-exponential curve. Results are summarized in Table 2. The time course of the fluorescence intensity of AEDANS-1-Tn or AEDANS-181-Tn on thin filaments reconstituted with nonlabeled F actin (in the absence of the acceptor) was also followed from $-Ca^{2+}$ to $+Ca^{2+}$ (or vice versa) under the same experimental conditions. However, in this case, the fluorescence intensity change was not appreciably seen.

Kinetics of S1-Induced Movement of TnI. Steady-state FRET measurements showed that rigor S1 binding to the regulated thin filament induces the open state, and the transfer efficiency between probes attached to TnI and actin decreases during the transition (the fluorescence intensity of the donor increases). Time courses of light-scattering and fluorescence intensity changes of the reconstituted thin filament were followed in the presence of Ca^{2+} after S1 binding or dissociation (transition from closed to open states or vice versa). Figure 3 shows the case of thin filaments reconstituted with AEDANS-133-Tn and DAB-F-actin. In the case of S1 dissociation, the reconstituted thin filaments and S1 complex in buffer F_{+Ca} was rapidly mixed with the same volume of buffer F_{+Ca} containing 1.0 mM ATP at 20 °C. The light-scattering and fluorescence intensity changes were analyzed with a single-exponential curve of which the rate constants were 868 ± 76 s^{-1} (Figure 3A-1) and 216 ± 42 s^{-1} (Figure 3A-2), respectively. In the case of S1 binding, the reconstituted thin filament in 140 mM KCl, 2 mM $MgCl_2$, 20 mM MOPS (pH 7.5), 1 mM NaN_3, and 0.1 mM $CaCl_2$ (buffer F'_{+Ca}) was rapidly mixed with the same volume of S1 in buffer F'_{+Ca} at 20 °C. When S1 was mixed with thin filaments, the fluorescence intensity increased simultaneously with light scattering (Figure 3B-1 and 3B-2). The curves were fitted with a single-exponential process of which the rate constants were 9.53 ± 1.24 s^{-1} for light scattering and 9.04 ± 1.18 s^{-1} for fluorescence.

Time courses of light-scattering and fluorescence intensity changes of the reconstituted thin filament were followed also in the absence of Ca^{2+} after S1 binding or dissociation (transition from the locked to open states or vice versa). In the case of S1 dissociation (Figure 4A), the reconstituted thin filament and S1 complex in 30 mM KCl, 2 mM $MgCl_2$, 20 mM MOPS (pH 7.5), 1 mM NaN_3, and 0.5 mM EGTA (buffer F_{-Ca}) was mixed with the same volume of buffer F_{-Ca} containing 1.0 mM ATP at 20 °C. The light-scattering intensity change was analyzed by a single-exponential decay (Figure 4A-1) with the rate constant of 997 ± 83 s^{-1}. On the other hand, the fluorescence intensity change was fitted by a double-exponential decay curve (Figure 4A-2) with the rate constants of 360 ± 44 and 44.9 ± 5.7 s^{-1}. The

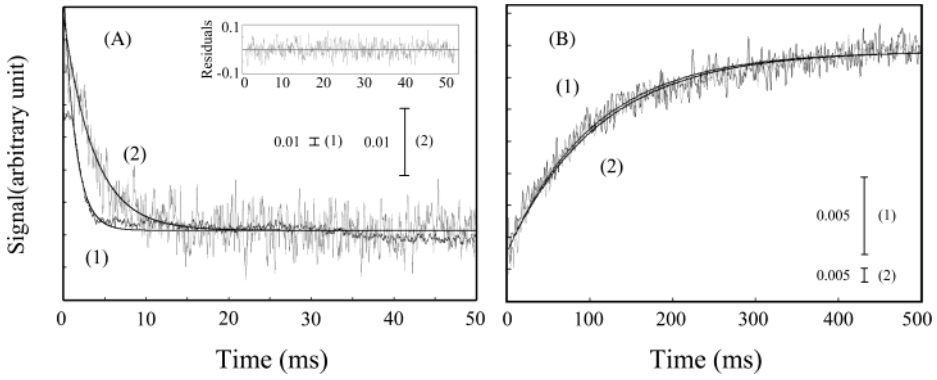

FIGURE 3: Stopped-flow traces for the S1-induced TnI movement in the presence of Ca^{2+} on the reconstituted thin filament. Stopped-flow signals were followed by light scattering (curve 1) or fluorescence intensity change (curve 2). (A) A total of 4.7 μM F actin, 0.67 μM Tm, 0.64 μM Tn, and 4.8 μM S1 in buffer F_{+Ca} were mixed with buffer F_{+Ca} + 1 mM ATP. (B) A total of 2.4 μM F actin, 0.33 μM Tm, and 0.32 μM Tn in buffer F'_{+Ca} were mixed with 9.6 μM S1 in buffer F'_{+Ca}. The best-fit exponential curve to each trace was superimposed. The inset of A shows the residual plot for the fitting of curve 2.

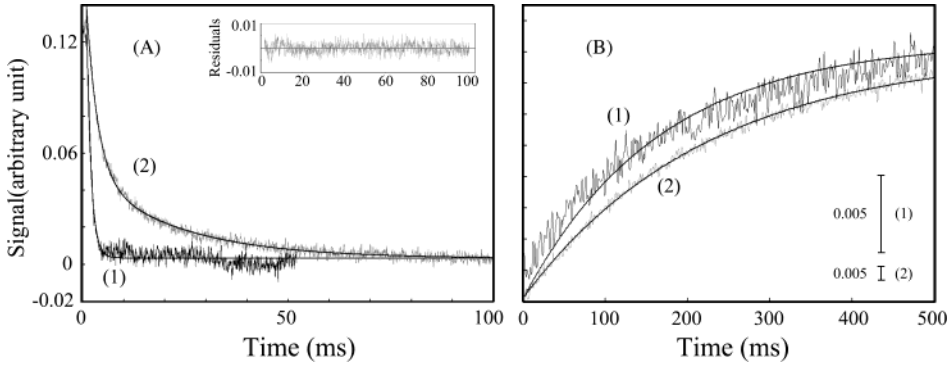

FIGURE 4: Stopped-flow traces for the S1-induced TnI movement in the absence of Ca^{2+} on the reconstituted thin filament. Sample and experimental conditions were the same as described in Figure 3, except for 1 mM EGTA instead of 0.1 mM $CaCl_2$ in buffer solutions. S1 dissociation (A) or S1 binding (B) was traced with light-scattering (curve 1) or fluorescence (curve 2) signals. The best-fit exponential curve to each trace was superimposed. The inset of A shows the residual plot for the fitting of curve 2.

Table 3: Rate Constants of the Transition between States of Thin Filaments Induced by S1 Binding/Dissociation[a]

	S1 dissociation			S1 binding	
donor site of TnI	k_{LS} (s^{-1})	k_{FL} (s^{-1})		k_{LS} (s^{-1})	k_{FL} (s^{-1})
(+Ca^{2+})					
TnIG1C	942 ± 75	330 ± 39		8.94 ± 1.16	8.75 ± 1.14
TnICys133	868 ± 76	216 ± 42		9.53 ± 1.24	9.04 ± 1.18
TnIS181C	825 ± 68	384 ± 67		8.91 ± 1.16	8.36 ± 1.09
donor site of TnI	k_{LS} (s^{-1})	k_{FL1} (s^{-1})	k_{FL2} (s^{-1})	k_{LS} (s^{-1})	k_{FL} (s^{-1})
(−Ca^{2+})					
TnIG1C	991 ± 89	549 ± 27 (0.79)	134 ± 6.2 (0.21)	4.74 ± 0.62	4.52 ± 0.59
TnICys133	997 ± 83	360 ± 44 (0.75)	44.9 ± 5.7 (0.25)	6.05 ± 0.79	4.50 ± 0.59
TnIS181C	836 ± 62	388 ± 93 (0.69)	43.9 ± 3.6 (0.31)	5.96 ± 0.77	6.09 ± 0.79

[a] Parentheses indicate the amplitude of the two rate constants.

fluorescence intensity change occurs much slower than the light-scattering change, indicating that, after S1 dissociation, TnI movement occurs with two steps. It should be mentioned here that the faster and slower rate constants of fluorescence intensity change are comparable to those of fluorescence intensity changes observed in Figure 3A (from the open to closed states) and in Figure 2C (from the closed to locked states), respectively.

In the case of S1 binding (Figure 4B), the reconstituted thin filament in 140 mM KCl, 2 mM $MgCl_2$, 20 mM MOPS (pH 7.5), 1 mM NaN_3, and 1 mM EGTA (buffer F'_{-Ca}) was rapidly mixed with the same volume of S1 in buffer F'_{-Ca} at 20 °C. In the absence of Ca^{2+}, the light-scattering transient showed an initial lag following by an approximately exponential phase as reported previously (*12*, *29*), which was interpreted in terms of an additional state of the thin filament that inhibits the initial binding of S1, the blocked state (*10*). When the initial lag phase for the light-scattering transient was neglected, curves were fitted by a single-exponential process with the rate constants of 6.05 ± 0.79 s^{-1} for light scattering and 4.50 ± 0.59 s^{-1} for fluorescence.

The time course of the fluorescence intensity of AEDANS-133-Tn on thin filaments reconstituted with nonlabeled F actin (in the absence of acceptor) was also followed after S1 binding or dissociation under the same experimental conditions. However, in this case, the fluorescence intensity change was not appreciably seen.

Time courses of light-scattering and fluorescence intensity changes of AEDANS-1-Tn and AEDANS-181-Tn were also followed by the stopped-flow apparatus after S1 binding or dissociation in the presence and absence of Ca^{2+}. Almost

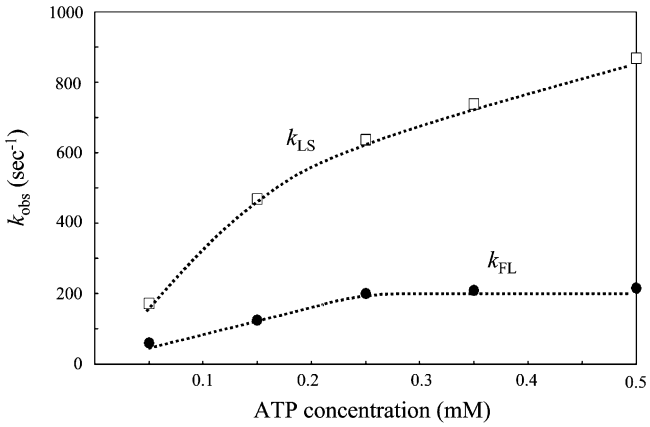

FIGURE 5: Effect of the ATP concentration on the rate constants of S1-induced conformational change in the presence of Ca^{2+}. Experimental conditions were the same as in Figure 3 (A), except for the ATP concentration. The rate constants are plotted against the ATP concentration after rapid mixing.

the same results as the case of AEDANS-131-Tn were obtained. The results are summarized in Table 3.

Effects of ATP Concentrations on Rate Constants. Rate constants of scattering and fluorescence intensity changes of the reconstituted thin filament after S1 dissociation were determined at various ATP concentrations, using AEDANS-133-Tn. Stopped-flow measurements were carried out under the same conditions as shown in Figures 3A and 4A except for the concentration of ATP. Figures 5 and 6 show the rate constants of scattering and fluorescence intensity changes of the reconstituted thin filament after S1 dissociation versus ATP concentration in the reaction mixture, in the presence

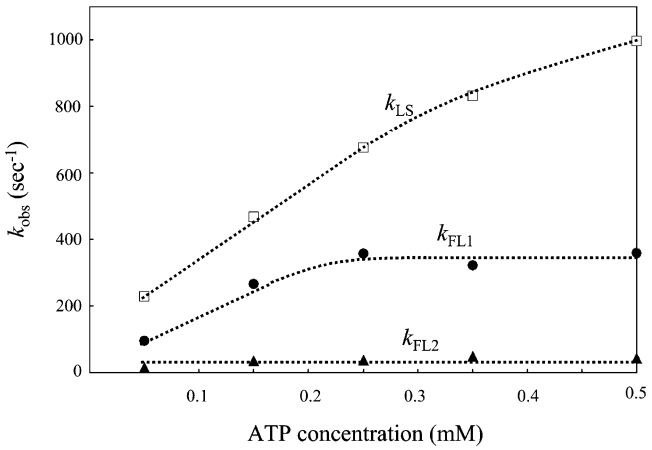

FIGURE 6: Effect of the ATP concentration on the rate constants of S1-induced conformational change in the absence of Ca^{2+}. Experimental conditions were the same as in Figure 4 (A), except for the ATP concentration. The rate constants are plotted against the ATP concentration after rapid mixing.

and absence of Ca^{2+}, respectively. The rate constant of scattering intensity change (dissociation of S1 from the thin filament) increased markedly as ATP concentration increased both in the presence and absence of Ca^{2+}. Time courses of fluorescence intensity change after S1 dissociation were analyzed with one rate constant (k_{FL}) in the presence of Ca^{2+} (transition from the closed to locked states) and two rate constants (k_{FL1} and k_{FL2}) in the absence of Ca^{2+} (transition from the open to locked states). k_{FL1} increased significantly as the ATP concentration increased up to 0.25 mM but did not change at more than 0.25 mM ATP. k_{FL2} did not appreciably depend on the ATP concentration. On the other hand, k_{FL} was almost the same as k_{FL1} and showed the same dependency on the ATP concentration as k_{FL1}.

DISCUSSION

Three States of Thin Filaments. In previous FRET measurements between TnI and actin, Cys-133 of TnI was labeled (*24*). In the present study, the N- and C-termini of TnI were selectively labeled by using point-mutated TnI. These residues are separated from each other on TnI according to the crystal structure of the core domain of Tn (*36*). These sites also showed Ca^{2+}- and S1-induced movements, although the extent of movement was smaller than that of Cys-133 (Table 1). The present results showed that not only the regulatory region but also whole TnI moves on the thin filament in response to the three states of the thin filament. Plots of the changes in fluorescence intensity versus the molar ratio of S1/actin showed a hyperbolic curve in the presence of Ca^{2+}, while it showed a sigmoidal curve in the absence of Ca^{2+}, as reported previously with Cys-133 of TnI, and Cys-60 or Cys-250 of TnT (*24*, *26*). This indicates that single S1 rigor binding on a unit length of a thin filament is enough to induce the open state in the presence of Ca^{2+}, but several S1 rigor bindings on a unit length are required in the absence of Ca^{2+}. In the presence of MgATP, the probability of the several strongly bound S1 molecules existing on a unit length of a thin filament is extremely small, resulting in the inhibition of acto-S1 ATPase activity in the absence of Ca^{2+}. On the other hand, in the presence of Ca^{2+}, single S1 on a unit length of a thin filament can induce the transition, and consequently, the cycle of ATPase turns smoothly.

Transition Rates of Ca^{2+}-Induced TnI Movement. In our previous paper (*21*), Cys-133 on TnI was labeled with 4-acetamino-4′-maleimidylstilbene-2,2′-disulfonic acid (AMS), and Lys-61 on actin was labeled with fluorescein 5-isothiocyanate. FRET between these probes in combination with stopped-flow methods gave the transition rates of Ca^{2+}-induced movement of TnI. The transition rate from the locked to closed states was 530 ± 170 s^{-1}, and the reverse rate was 43 ± 5 s^{-1}. In the present study, the positions 1 and 181 on TnI were labeled with IAEDANS, and Cys-374 on actin was labeled with DABMI. As shown in Table 2, the transition rates measured by using these sites were almost the same as those in the previous report (*21*), suggesting that TnI moves not sequentially step by step but synchronously as a whole. This is consistent with the recent report by Dong et al. (*37*). Using FRET in combination with stopped-flow methods, they measured the rates of three conformational transitions in cardiac Tn induced by Ca^{2+} dissociation from TnC: (1) closing of the TnC N domain, (2) decrease in the end-to-end separation of the inhibitory region of TnI, and (3) separation of TnI from TnC in the central helix region of TnC. These three transitions occur with very similar rates. On the other hand, the fluorescence intensity change of probes attached to Met-25 on TnC (*38*) or Cys-133 of TnI (*21*) in the absence of the acceptor finished within the instrumental dead time (4 ms) when the free Ca^{2+} concentration was abruptly increased. The fluorescence intensity change in the absence of the acceptor indicates an environmental change around the probe but does not necessary mean a spatial rearrangement of thin filaments. Ca^{2+} can bind to the Ca^{2+}-specific sites of TnC with the rate constant of $(1-2) \times 10^8$ M^{-1} s^{-1} at 4 °C (*39*). Upon Ca^{2+} binding to TnC, the information spreads in a whole troponin complex with a rate constant much higher than 750 s^{-1}. This rapid conformational change causes a change of the spatial rearrangement of troponin, and consequently, TnI as a whole goes away from the actin filament with a rate constant of several hundreds per seconds. When the free Ca^{2+} concentration was abruptly decreased, TnI moves toward the outer domain of actin with a rate constant of several tens per seconds. The time-scale measurements of Ca^{2+}-induced spatial rearrangement of thin filaments observed by FRET were in good correlation with those measured from time-resolved X-ray diffraction of a contracting frog muscle (*40*).

Transition Rates of S1-Induced TnI Movement. Geeves and his colleagues (*11*, *27*, *28*) carried out stopped-flow measurements based on the three-state model. The rate of change in state was monitored by the fluorescence intensity of a pyrene label attached to Tm or actin. These rates were compared with those of S1 binding or the dissociation measured by light scattering. When the fluorescence intensity change of the pyrene label attached to Tm was monitored (*11*), they showed that the transition from the open to closed or relaxed states seemed to occur with a much slower rate constant than the present rate constant, and the rate did not depend on Ca^{2+} concentrations. However, the change in fluorescence intensity indicates an environmental change around the fluorescence probe, but does not necessarily mean a spatial rearrangement of thin filaments. Only from the fluorescence intensity change, it is difficult to assign what kind of conformational change occurred. FRET in combination with stopped-flow methods can determine the rate of spatial rearrangement of

thin filaments. The fluorescence intensity of the energy donor is often sensitive to its environment. The environmental sensitivity of the donor would contribute to the transition rates measured by stopped-flow measurements. However, the energy donor used in the present stopped-flow measurements was not sensitive to its environment. Therefore, the observed changes in fluorescence intensity by stopped-flow measurements could be attributed to the change in FRET efficiency.

When bound S1 was abruptly dissociated from regulated thin filaments in the presence of Ca^{2+}, a transition from the open to closed states occurs. Light scattering showed that S1 dissociation occurs with a rate constant of ~900 s^{-1}. FRET showed that TnI movement from the open to closed states occurs with a rate constant of ~300 s^{-1} (Table 3). Figure 5 shows the dependency of rate constants on the ATP concentration. The rate constant for S1 dissociation increased as the ATP concentration increased. On the other hand, the rate constant for TnI movement increased as the ATP concentration increased up to 0.25 mM, but it became constant over the 0.25 mM ATP concentration. When bound S1 was abruptly dissociated from regulated thin filaments in the absence of Ca^{2+}, a transition from the open to locked state is supposed to occur. Light scattering showed that S1 dissociation occurs with a rate constant of ~950 s^{-1}. FRET showed that TnI movement occurs with two rate constants of ~400 and ~80 s^{-1} (Table 3). The faster rate constant k_{FL1} is compatible to that for the transition from the open to closed states observed in the presence of Ca^{2+}. On the other hand, the slower rate constant k_{FL2} is similar to that for the transition from the closed to locked states as shown in Table 2. These results indicate that the transition occurs in two steps, from the open to closed states and then from the closed to locked states. Figure 6 shows the dependency of rate constants on the ATP concentration in the absence of Ca^{2+}. The rate constant for S1 dissociation increased as the ATP concentration increased as described in the presence of Ca^{2+}. The faster rate constant for TnI movement increased as the ATP concentration increased up to 0.25 mM, but it became constant over the 0.25 mM ATP concentration. On the other hand, the slower rate constant did not significantly depend on the ATP concentration. These can be explained as the following equations.

$$\begin{array}{ccccc} A^* & & & & \\ \updownarrow & & & & \\ B^* & \xrightarrow{k_1} & C & \xrightarrow{k_2} & D \end{array}$$

Here, the sum of A* and B* is the open state, C is the closed state, and D is the locked state. There is a rapid equilibrium between A* and B*, and strong S1 binding stabilizes the state A*. ATP dissociates the strong bound S1 from the thin filament. Thus, the equilibrium constant between A* and B* depends on the ATP concentration.

$$[B^*]/[A^*][ATP] = K'$$

$$d([A^*] + [B^*])/dt = -k_1[B^*] = -k_1K'[ATP]([A^*] + [B^*])/(1 + K'[ATP])$$

$$[A^*] + [B^*] \propto \exp\{-k_1K'[ATP]t/(1 + K'[ATP])\}$$

In the stopped-flow experiments of S1 dissociation by ATP (Figures 3−6), the initial state of the thin filament is 100% A*. After rapid mixing with the ATP solution, strongly bound S1 rapidly dissociates from the thin filament depending on the concentration of ATP, following the increase of the population of B*. Then, the transitions to C and D start. When the concentration of ATP becomes a sufficient amount, the observed rate constant k_{FL} $\{=k_1K'[ATP]/(1 + K'[ATP])\}$ becomes k_1 and does not depends any more on the ATP concentration. Because the transition rate from A*, through B*, to C is 1 order faster than the transition rate from C to D, the transition from A* to B* does not effect the rate constant of k_2. Although the present model provides reasonable explanation for the dependency of the rate constants on the ATP concentration, it may be too simplified. A more refined model, taking into account the cooperativity of S1 binding, would be necessary. FRET in combination with stopped-flow methods clearly determined the rate constants for transitions from the open to closed states and from the closed to locked states. These rate constants are fast enough for the three states of thin filaments to be directly involved in the regulation mechanism.

When the regulated thin filament was rapidly mixed with S1 in the presence of Ca^{2+}, a transition from the closed to open states after S1 binding is supposed to occur. Light scattering showed that S1 binding occurs with a rate constant of ~9 s^{-1}. FRET showed that TnI movement occurs with almost the same rate constant as S1 binding (Table 3). The transition from the closed to open states is supposed to occur within several milliseconds after S1 binding. On the other hand, when the regulated thin filament was rapidly mixed with S1 in the absence of Ca^{2+}, a transition from the locked to open states after S1 binding is supposed to occur. Light-scattering measurements showed that S1 binding occurs with a rate constant of ~5 s^{-1}. The rate constant of S1 binding to regulated thin filaments in the absence of Ca^{2+} was slower than that in the presence of Ca^{2+}, in accordance with previous reports (*11*, *29*). Geeves and Lehrer (*11*) measured the rate of transition between the three states of thin filaments by monitoring fluorescence intensity from the pyrene label attached to Tm. Their rate constants observed by light scattering were comparable to the present data, but in contrast to our FRET measurements, the rate of fluorescence intensity change of pyrene on Tm was 1 order faster than the rate of scattering light change both in the presence and absence of Ca^{2+}. Present FRET measurements showed a slightly slower rate for the transition from the locked to open states than the rate of S1 binding (Table 3). However, these data are not incompatible with each other. The binding of S1 induces a cooperative conformational change of actin subunits through Tm, and the fluorescence intensity of pyrene on Tm increased very quickly. This conformational change follows a spatial rearrangement of thin filaments in which TnI detaches further away from the outer domain of actin at a 1 order slower rate.

ACKNOWLEDGMENT

We appreciate the assistance of Mr. Koichi Misawa for stopped-flow measurements at an early stage and thank Dr. Kayo Maeda for her kind help in preparation of mutant TnI.

REFERENCES

1. Ebashi, S., Endo, M., and Ohtsuki, I. (1969) Control of muscle contraction, *Q. Rev. Biophys. 2*, 351−384.
2. Ohtsuki, I., and Wakabayashi, T. (1972) Optical diffraction studies on the structure of troponin−tropomyosin−actin paracrystals, *J. Biochem. 72*, 369−377.
3. Ohtsuki, I., Maruyama, K., and Ebashi, S. (1986) Regulatory and cytoskeletal proteins of vertebrate skeletal muscle, *Adv. Protein Chem. 38*, 1−67.
4. Farah, C. S., and Reinach, F. C. (1995) The troponin complex and regulation of muscle contraction, *FASEB J. 9*, 755−767.
5. Gordon, A. M., Homsher, E., and Regnier, M. (2000) Regulation of contraction in striated muscle, *Physiol. Rev. 80*, 853−924.
6. Chalovich, J. M. (1992) Actin mediated regulation of muscle contraction, *Pharmacol. Ther. 55*, 95−148.
7. Tobacman, L. S. (1996) Thin filament-mediated regulation of cardiac contraction, *Annu. Rev. Physiol. 58*, 447−481.
8. Huxley, H. E. (1972) Structural changes in the actin and myosin containing filaments during contraction, *Cold Spring Harbor Symp. Quant. Biol. 37*, 361−376.
9. Haselgrove, J. (1972) X-ray evidence for a conformational change in the actin containing filaments of vertebrate striated muscle, *Cold Spring Harbor Symp. Quant. Biol. 37*, 341−352.
10. Mckillop, D. F., and Geeves, M. A. (1993) Regulation of the interaction between actin and myosin subfragment 1: Evidence for three states of the thin filament, *Biophys. J. 65*, 693−701.
11. Geeves, M. A., and Lehrer, S. S. (1994) Dynamics of the muscle thin filament regulatory switch: the size of the cooperative unit, *Biophys. J. 67*, 273−282.
12. Lehrer, S. S., and Geeves, M. A. (1998) The muscle thin filament as a classical cooperative/allosteric regulatory system, *J. Mol. Biol. 277*, 1081−1089.
13. Holmes, K. C. (1995) The actomyosin interaction and its control by tropomyosin, *Biophys. J. 68* (suppl.), 2−7.
14. Vibert, P., Craig, R., and Lehman, W. (1997) Steric-model for activation of muscle thin filamenents, *J. Mol. Biol. 266*, 8−14.
15. Squire, J. M., and Morris, E. P. (1998) A new look at thin filament regulation in vertebrate skeletal muscle, *FASEB J. 12*, 761−771.
16. Stryer, L. (1978) Fluorescence energy transfer as a spectroscopic ruler, *Annu. Rev. Biochem. 47*, 819−846.
17. dos Remedios, C. G., Miki, M., and Barden, J. A. (1987) Fluorescence resonance energy transfer measurements of distances in actin and myosin. A critical evaluation, *J. Muscle Res. Cell Motil. 8*, 97−117.
18. Miki, M., O'Donoghue, S. I., and dos Remedios, C. G. (1992) Structure of actin observed by fluorescence resonance energy transfer spectroscopy, *J. Muscle Res. Cell Motil. 13*, 132−145.
19. Miki, M. (1990) Resonance energy transfer between points in a reconstituted skeletal muscle thin filament: A conformational change of the thin filament in response to a change in Ca^{2+} concentration, *Eur. J. Biochem. 187*, 155−162.
20. Tao, T., Gong, B. J., and Leavis, P. C. (1990) Calcium-induced movement of troponin-I relative to actin in skeletal muscle thin filaments, *Science 247*, 1339−1341.
21. Miki, M., and Iio, T. (1993) Kinetics of structural changes of reconstituted skeletal muscle thin filaments observed by fluorescence resonance energy transfer, *J. Biol. Chem. 268*, 7101−7106.
22. Miki, M., Kobayashi, T., Kimura, H., Hagiwara, A., Hai, H., and Maéda, Y. (1998) Ca^{2+}-induced distance change between points on actin and troponin in skeletal muscle thin filaments estimated by fluorescence energy transfer spectroscopy, *J. Biochem. 123*, 324−331.
23. Kobayashi, T., Kobayashi, M., and Collins, J. H. (2001) Ca^{2+}-dependent, myosin subfragment 1-induced proximity changes between actin and the inhibitory region of troponin I, *Biochim. Biophys. Acta 1549*, 148−154.
24. Hai, H., Sano, K., Maeda, K., Maéda, Y., and Miki, M. (2002) Ca^{2+}-induced conformational change of reconstituted skeletal muscle thin filaments with an internal deletion mutant D234-tropomyosin observed by fluorescence energy transfer spectroscopy: Structural evidence for three states of thin filament, *J. Biochem. 131*, 407−418.
25. Landis, C. A., Bobkova, A., Homsher, E., and Tobacman, L. S. (1997) Effects of tropomyosin internal deletions on thin filament function, *J. Biol. Chem. 272*, 14051−14056.
26. Kimura, C., Maeda, K., Maéda, Y., and Miki, M. (2002) Ca^{2+}- and S1-induced movement of troponin T on reconstituted skeletal muscle thin filaments observed by fluorescence energy transfer spectroscopy, *J. Biochem. 132*, 93−102.
27. Maytum, R., Lehrer S. S., and Geeves M. A. (1999) Cooperativity and switching within the three-state model of muscle regulation, *Biochemistry 19*, 1102−1110.
28. Maytum, R., Geeves M. A., and Lehrer S. S. (2002) A modulatory role for the troponin T tail domain in thin filament regulation, *J. Biol. Chem. 277*, 29774−29780.
29. Resetar, A. M., Stephens, J. M., and Chalovich, J. M. (2002) Troponin−tropomyosin: An allosteric switch or a steric blocker? *Biophys. J. 83*, 1039−1049.
30. Kluwe, L., Maeda, K., and Maéda, Y. (1993) *E. coli* expression and characterization of a mutant troponin I with the three cysteine residues substituted, *FEBS Lett. 323*, 83−88.
31. Lamkin, M., Tao, T., and Lehrer, S. S. (1983) Tropomyosin−troponin and tropomyosin−actin interactions: A fluorescence quenching study, *Biochemistry 22*, 3053−3058.
32. Hudson, E. N., and Weber, G. (1973) Synthesis and characterization of two fluorescent sulfhydryl reagents, *Biochemistry 12*, 4154−4161.
33. Lakowicz, J. R. (1999) *Principles of Fluorescence Spectroscopy*, 2nd ed., Kluwer Academic/Plenum Publishers, New York.
34. Scott, T. G., Spencer, R. D., Leonard, N. G., and Weber, G. (1970) Emission properties of NADH. Studies of fluorescence lifetimes and quantum efficiencies of NADH, AcPyADH, and simplified synthetic models, *J. Am. Chem. Soc. 92*, 687−695.
35. Tausky, H. H., and Shorr, E. (1953) A microcolorimetric method for the determination of inorganic phosphorus, *J. Biol. Chem. 202*, 675−685.
36. Takeda, S., Yamashita, A., Maeda, K., and Maéda, Y. (2003) Structure of the core domain of human cardiac troponin in the Ca^{2+}-saturated form, *Nature 424*, 35−41.
37. Dong, W. J., Robinson, J. M., Xing, J., and Cheung, H. C. (2003) Kinetics of conformational transitions in cardiac troponin induced by Ca^{2+} dissociation determined by Förster resonance energy transfer, *J. Biol. Chem. 278*, 42394−42402.
38. Iio, T., Nishio, Y., and Kondo, H. (1988) Fluorescence titration and fluorescence stopped-flow studies of skeletal muscle troponin-nonpolymerizable tropomyosin complex, *J. Biochem. 104*, 306−311.
39. Johnson, J. D., Nakkula, R. J., Vasulka, C., and Smillie, L. B. (1994) Modulation of Ca^{2+} exchange with the Ca^{2+}-specific regulatory sites of troponin C, *J. Biol. Chem. 269*, 8919−8923.
40. Kress, M., Huxley, H. E., Faruqi, A. R., and Hendrix, J. (1986) Structural changes during activation of frog muscle studied by time-resolved X-ray diffraction, *J. Mol. Biol. 188*, 325−342.

BI0492713